Applied Geochemistry 97 (2018) 147–156

Contents lists available at ScienceDirect

Applied Geochemistry

journal homepage: www.elsevier.com/locate/apgeochem

Coupling of chemical and hydromechanical properties in bentonite

A. Jenni*, U. Mäder

RWI, Institute of Geological Sciences, University of Bern, Baltzerstrasse 3, CH-3012, Bern, Switzerland

ARTICLE INFO

Editorial handling by Adrian Bath

Keywords:
Bentonite
Electrostatic porosity concepts
Swelling pressure
Hydraulic conductivity
Porosity distribution
Reactive transport modelling
HMC coupling

ABSTRACT

Bentonite plays a key role as buffer/backfill in many engineered barrier concepts for nuclear waste repositories and is required to perform over long periods of time. Swelling pressure and porosity distribution, two of the crucial properties for the performance of bentonite, vary with the chemical environment. This contribution reviews available data, explores a simple coupling model, and applies it to a fresh water/saline water scenario.

Systematic swelling pressure data for bentonite or montmorillonite under controlled chemical conditions are scarce. Evaluation of literature data shows that swelling pressure drops by 75% when increasing ionic strength of the equilibrated NaCl electrolyte from 0 to 3 M for an effective montmorillonite dry density corresponding to 1500 kg/m^3 (MX-80 bentonite). In contrast, swelling pressure of $CaCl_2$-equilibrated montmorillonite drops only by 40% for the same ionic strength increase. Cation occupancy strongly affects swelling pressure at densities below 1500 kg/m^3 (monovalent vs. divalent), and ionic strength still controls swelling pressure at higher density.

The chemical influence on the pore size/shape distribution in confined constant-volume systems is poorly investigated. The presence and quantity of a "free" porosity containing charge-balanced electrolyte (not affected by charged clay surfaces) in highly compacted clay systems is debated. Experimental data states different average montmorillonite interlayer distances at different ionic strengths at constant dry density. Assuming a constant volume for solids and electrolyte, any change in interlayer volume must be compensated by a corresponding change in some other type of porosity, most likely in a larger-size porosity domain. This coupling of ionic strength to porosity can explain differences in advective and diffusive transport commonly observed in clays tested with different background electrolyte concentrations, but at the same density.

The existence of any effect of cation occupancy on porosity distribution has not been confirmed so far. Observed differences in advective and diffusive solute transport between Na and Ca montmorillonite might be caused by different microstructures originating from sample preparation. However, our own experimental approach avoiding such artefacts also results in transport properties dependent on the exchanger cation.

Own and critically reviewed data from literature indicate a coupling of ionic strength or cation occupancy with porosity distribution. The influence of ionic strength is stronger and supported by experimental data. This HMC coupling (hydromechanical-chemical) was incorporated into a dual-porosity multicomponent reactive transport code. The code maps the complex porosity distribution into two domains: the *Donnan porosity* contains the porewater influenced by the negatively charged clay sheet surfaces, and has to compensate for this permanent charge with cations (representing the exchangeable cations of the clay). The Donnan porosity comprises clay interlayers and a region near clay particle outer surfaces (diffuse double layer). The Donnan porewater composition is at equilibrium with the charge-balanced "*free porewater*" not affected by surface charge. Both, the interlayer distance and the thickness of the diffuse double layer are assumed to depend linearly on the Debye length (dependent on ionic strength).

Two reactive transport modelling examples show that equilibration time of bentonite with different ionic strength waters varies significantly. The redistribution of porosity slows down or accelerates diffusive transport.

1. Introduction

Many studies demonstrate an influence of the bentonite's porewater chemistry on swelling pressure, hydraulic conductivity, and porosity distribution (references provided below). In the context of bentonite used as buffer around radioactive waste canisters or as sealing

* Corresponding author.
E-mail addresses: andreas.jenni@geo.unibe.ch (A. Jenni), urs.maeder@geo.unibe.ch (U. Mäder).

https://doi.org/10.1016/j.apgeochem.2018.08.013
Received 29 March 2018; Received in revised form 14 August 2018; Accepted 20 August 2018
Available online 23 August 2018
0883-2927/

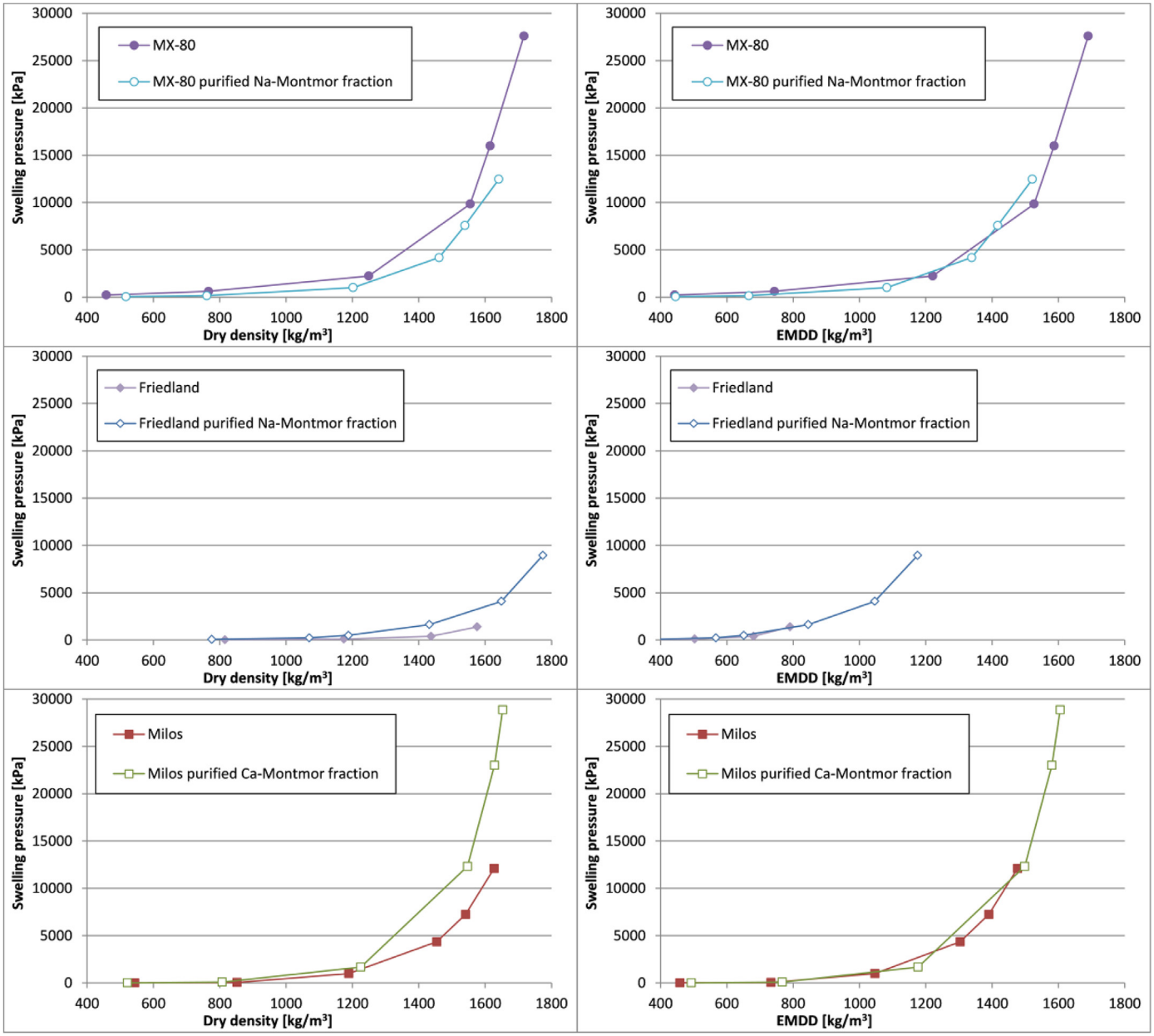

Fig. 1. Swelling pressures of three different bentonites and of their purified montmorillonite fraction are plotted against bulk dry density (left) and EMDD (right). Data is taken from Karnland et al. (2006). Lines are shown for better readability.

components, the main transport properties, hydraulic conductivity and diffusivity, are crucial for limiting the interaction with other materials in the near-field (e.g., steel, host rock, cement, or the waste itself). The porosity distribution is one key parameter that constrains conductivity and diffusivity. Porosity changes do not only slow down or accelerate transport, but can virtually stop the interaction at an interface (porosity clogging). In addition, swelling pressure is a safety-relevant bentonite property for the mechanical performance of a repository. Therefore, the swelling pressure evolution during the life-time of a repository should be known.

The relationship between transport in bentonite and swelling pressure is still not quantitatively understood. In general, an inverse behaviour can be observed. Swelling pressures of saturated bentonite reported in the literature differ substantially (Karnland, 2010; Kaufhold et al., 2015; Kumpulainen and Kiviranta, 2011). Data is commonly presented in plotting swelling pressure against dry density, the latter being the most important bentonite property influencing its swelling pressure. Comparison of such curves reveals that additional bentonite properties influence swelling pressure:

- *Accessory mineral content* influences dry density significantly. Fig. 1 shows that swelling pressure-dry density curves of bentonites and their purified homo-ionic clay fractions differ from each other significantly. If pressure is plotted against the effective montmorillonite dry density (EMDD, Dixon et al., 2002), both curves merge. This holds true for bentonites with low and high accessory contents (Wyoming/MX-80 and Milos: 15–20 wt%, Friedland: 60–70 wt%), as well as for Na-bentonites (MX-80, Friedland) and Ca-bentonites (Milos). The EMDD can be seen as dry density of the montmorillonite matrix in between the accessory minerals and is calculated as

$$\delta_{EMdry} = \frac{f_{Mm} \cdot \delta_{dry}}{1 - ((1 - f_{Mm}) \cdot \delta_{dry} / \delta_{acc}} \quad (1)$$

with f_{Mm} representing the montmorillonite mass fraction, δ_{dry} the dry density of the mixture, and δ_{acc} the average accessory mineral density.
Recent studies confirm experimentally and theoretically that up to 40–50% of homogenously distributed inert filler do not affect swelling pressure (unpublished data summary by Ola Karnland). In order to compare influences of other montmorillonite properties on swelling pressures, they should be compared at equal EMDD and not at equal bulk dry density.

- *Smectite structure*: montmorillonite represents the swelling mineral in most bentonites. CEC/layer charge and the proportion of octahedral and tetrahedral charges influence the swelling behaviour of bentonite (Christidis et al., 2006; Güven, 1988; Meunier, 2005).
- *Microstructure* (grain sizes and morphologies, grain agglomerates and preferred orientations) influences swelling pressure evolution during saturation and homogenisation of the material (Seiphoori et al., 2014). The influence is smaller after completion of these transient processes.
- *Cation occupancy* of the clay exchanger and *ionic strength* in the free porosity influence transport properties and swelling pressure of the bentonite. Equilibration of external solutions with bentonite may require months or even years: accessory minerals (especially gypsum and carbonates) may control the composition of the free porewater in the bentonite as well as the exchanger population. Equilibrium is only reached when minerals that are unstable in the external solution have dissolved. This again decreases the dry density and therefore swelling pressure. In addition, equilibration of the cation occupancy of the exchanger with the external solution may require several pore volumes flushed through compacted bentonite (Jenni et al., 2014), or a correspondingly long time for diffusive exchange. This is rooted in the fact that the CEC comprises considerably more cations per volume of porous media than dissolved in an average porewater in the free porosity. Swelling pressure and transport measurements should be done only on clay samples in equilibrium with the external and pore solution.

This coupling between porewater chemistry and hydromechanical key parameters (HMC coupling) is explored in this article on the basis of literature data and own supplementary measurements. A reactive transport model exercise, including a first simplified HMC coupling approach, illustrates the importance of this coupling.

In the following, the porosity in fully saturated bentonite is divided into a *free porosity* far from the charged clay sheet surfaces (charge-balanced porewater, not affected by electrostatics), and a *Donnan porosity* influenced by negatively charged clay surfaces. This concept combines the Donnan porosity along clay grain outer surfaces and those within interlayers, because both types are influenced in a similar way by electrostatics. Applications of this concept can describe advective/diffusive solute transport through bentonite with two geometric factors (for Donnan and free porosity) used for all species (Alt-Epping et al., 2014). Advective solute transport is normally assumed to involve the free porosity only. The limited number of required parameters can be derived from experimental diffusion data. The comparatively simple concept allows for the simulation of complex reactive transport problems such as encountered across clay/cement interfaces (Jenni et al., 2017). This two-porosity concept merges with the homogenous Donnan concept of Birgersson and Karnland (2009) for diffusive transport when the free porosity becomes very small and the Donnan porosity dominant.

2. Background

If the host rock porewater adjacent to the bentonite changes during the lifetime of a repository, the porewater of the bentonite will be influenced. For example, a dilution of the external water in contact with the bentonite during a glaciation period provides a possible underlying scenario for such a case. Although a simultaneous and progressive alteration of the exchanger population is expected in a real scenario, this is kept constant in the selected experimental set-ups to avoid overlapping effects from two mechanisms (ionic strength and exchanger). For the same reason, dry density and total volume are also kept constant for all experimental data shown below.

2.1. Coupling of ionic strength to swelling pressure and porosity at constant volume/dry density and constant exchanger population

Literature studies of swelling pressure or measured montmorillonite layer thickness of bentonite equilibrated with electrolytes of specified ionic strength often neglect the controlling effect of soluble minerals present in the sample (e.g., Holmboe et al., 2012; Karnland et al., 2006 in case of unpurified bentonites). The contribution of mineral dissolution or even equilibration with atmospheric CO_2 should not be neglected, especially for external solutions intended to impose low ionic strength. For example, the 1 mM NaCl solution infiltrated into bentonite in the set-up of Holmboe et al. (2012) leads to a calculated porewater ionic strength of 44 mM in equilibrium with the known accessory minerals gypsum, calcite, and atmospheric CO_2. The steep slope of the swelling pressure-ionic strength curve close to zero ionic strength (Fig. 2) increases the significance of this issue: the swelling pressure is expected to be approximately 80 kPa lower at 44 mM NaCl compared to 0 M for 1500 kg/m^3 dry density. In contrast, sufficiently long equilibration time with near-constant reservoir chemistry removes all soluble accessory minerals, and the chemistry of the internal free pore water equals that of the external reservoir. But in this case, dry density is decreased due to mineral dissolution, which may significantly decrease swelling pressure, especially at high densities (Fig. 1). In case of the MX-80 disc described in chapter 3, dissolution of 1 vol% of gypsum decreases the EMDD from 1337 kg/m^3 to 1315 kg/m^3, and the swelling pressure is expected to drop from 3213 kPa to 2914 kPa (at equilibrium with 0.1 M NaCl). Measuring purified bentonite or pure montmorillonite avoids this issue. For a comparison of swelling pressure data at constant densities, the EMDD is relevant rather than bulk dry density.

Changes in ionic strength of the external solution influence osmotic swelling, which is generally assumed to occur only at low density (above approximately 19 Å interlayer distance). Therefore, strongest effects of changes in ionic strength on swelling pressures are measured at low densities (large interlayer distances) as shown in Fig. 3.

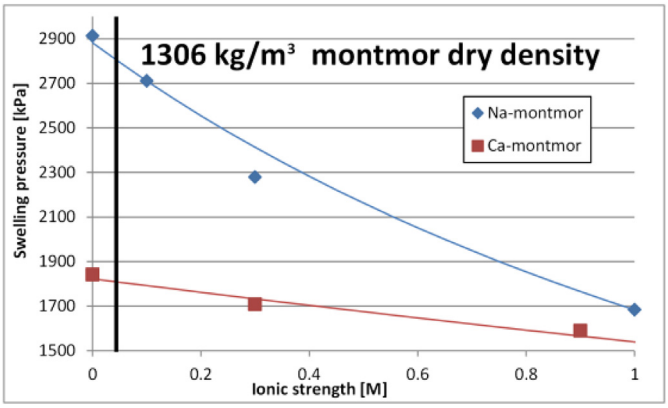

Fig. 2. Swelling pressure of Na-montmorillonite in NaCl and of Ca-montmorillonite in $CaCl_2$ solutions of different ionic strengths at 1306 kg/m^3 dry density. This montmorillonite dry density approximately corresponds to MX-80 bulk dry density of 1500 kg/m^3. Data from Karnland et al. (2006) was interpolated with exponential fit functions to estimate swelling pressures of Na- and Ca-montmorillonite at the desired density (data was originally measured at somewhat different densities). Lines represent least squares fits. The vertical line marks 44 mM ionic strength (see text).

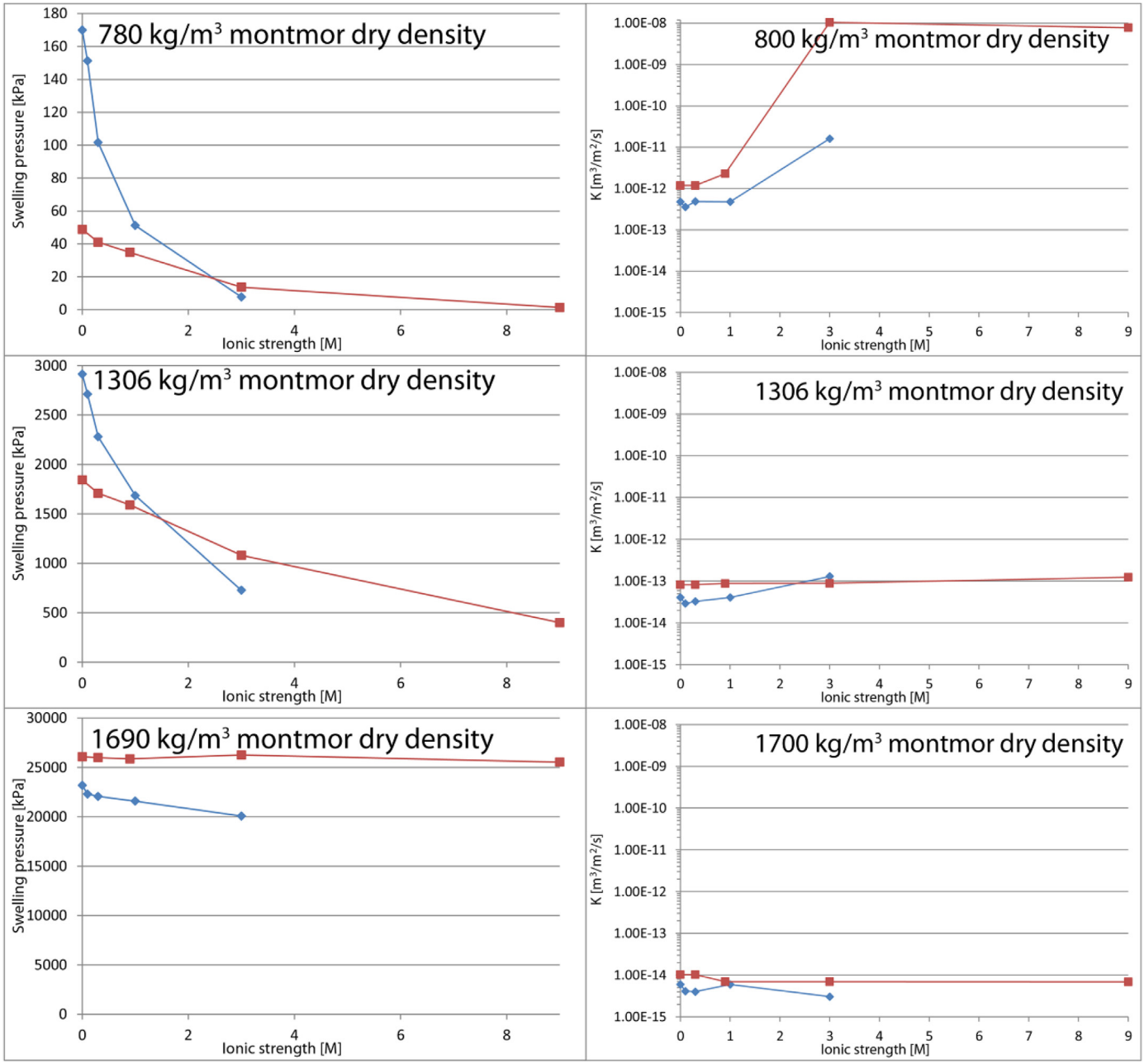

Fig. 3. Swelling pressure and hydraulic conductivity of Na-montmorillonite in NaCl (blue diamonds) and of Ca-montmorillonite in $CaCl_2$ (red squares) solutions of different ionic strengths at different dry density. The montmorillonite dry densities approximately correspond to MX-80 bulk dry densities of 950, 1500, and 1870 kg/m^3. Data from Karnland et al. (2006) was interpolated with exponential fit functions to estimate swelling pressures of Na- and Ca-montmorillonite at equal densities (data was originally measured at different densities). Lines are shown for better readability only. (For interpretation of the references to colour in this figure legend, the reader is referred to the Web version of this article.)

However, ionic strength also influences swelling pressures of highly compacted clays: Na-montmorillonite at 1690 kg/m^3 still shows a clear dependence of swelling pressure on ionic strength, whereas Ca-montmorillonite swelling pressure seems to remain constant (basal spacing around 15 Å). The influence of ionic strength on crystalline swelling, which is assumed to be responsible for swelling at this basal spacing, is not discussed in literature.

Direct observations of porosity distributions at different ionic strength but constant dry density are scarce. The XRD measurement of basal spacings in montmorillonite equilibrated with different NaCl concentrations clearly show the presence of 15.6 Å basal spacings (corresponding to two water layers) above 0.08 M NaCl (Kozaki et al., 2008). The corresponding XRD peak increases with increasing concentration up to 0.5 M NaCl. At 0.08 M NaCl or below, only basal spacings near 18.8 Å are observed (constant dry density of 1000 kg/m^3, corresponding to approximately 1185 kg/m^3 MX-80 bulk dry density). More recent measurements and more elaborate data processing indicate larger basal spacings of more than 30 Å at this density (Holmboe et al., 2012). The latter authors justify this large discrepancy of more than 10 Å with the data processing approach of Kozaki (simple use of Bragg's law instead of profile fitting), problems in water content determination, or material differences (larger particle size). However, the appearance of the two-water-layer basal distance (15.6 Å) only at higher ionic strength cannot be explained by such artefacts.

Ionic strength significantly influences the diffusion through clay materials. Glaus et al. (2010) report higher tracer Cl^- fluxes through

Na-montmorillonite (1900 kg/m^3 dry density) at higher ionic strengths. In line with the findings above, basal spacing in the montmorillonite is thought to decrease with higher ionic strength, and the decreasing Donnan porosity has to be compensated with a larger proportion of free porosity (total volume remains constant). The increasing free porosity is fully accessible to anions and must lead to a flux increase. Consistently, Van Loon et al. (2007) derive higher Cl^- diffusion accessible porosities for higher ionic strengths. This interpretation suggests the presence of a free porosity even at a high dry density of 1900 kg/m^3. However, it is based on a dual porosity assumption with a completely anion-free interlayer porosity and a homogeneous and connected charge-balanced porosity accessible for anion diffusion. The underlying data (aqueous extracts of bentonite after the diffusion experiments) can also be explained with a partly Cl^- accessible Donnan porosity and a charge-balanced free porosity, which leads to a smaller Cl^- accessible porosity than stated. Although the fluxes measured by Glaus et al. (2010) can be explained with this approach, it requires diffusive transport parameters for both Donnan and free porosities. Kozaki et al. (2008) measured cation diffusion in compacted smectite and derived higher apparent self-diffusion coefficients for $^{22}Na^+$ at higher ionic strength. Again, the authors explain this measurement with an increasing free porosity providing a faster pathway than the Donnan porosity. The authors further divided Donnan porosity water into montmorillonite grain surface water (often called DDL, diffuse double layer), and the interlayer water.

Ionic strength clearly influences hydraulic conductivity in montmorillonite (Fig. 3), confirmed by several additional studies (Chen et al., 2015; Zhu et al., 2013). In general, conductivity increases with higher ionic strength at constant dry densities up to around 1400 kg/m^3. At higher densities, and also in case of Ca-montmorillonite, this effect is less obvious or within the error of the method, which increases strongly at high densities (errors not stated by the author). This behaviour might also be explained with a decrease in interlayer distance at higher ionic strengths, which has to be compensated with an increasing free porosity. Permeability within the Donnan porosity can be expected to be several magnitudes smaller or even negligible compared to the free porosity. Alternative unpublished explanations argue that the clay surface – porewater interaction is influenced by its chemical composition. This interaction certainly influences the movement of polar water molecules along the charged clay sheet surface, and might be significant enough to influence hydraulic conductivity as a function of the carried ions. This would lead to an additional term in any kind of transport equation, and Darcy's law should not be valid anymore.

Hydraulic conductivity correlates exponentially with dry density (Karnland et al., 2006). Only in Ca-montmorillonite at very low swelling pressures (low dry densities and/or high ionic strengths), conductivity increases are above the prediction from the exponential function valid for higher dry densities. Coagulation of clay particles possibly leads to preferential flow pathways, and the material resembles rather a slurry than a compacted bentonite (e.g., hydraulic conductivities of 10^{-8} m/s in 800 kg/m^3 Ca-montmorillonite in 3 and 9 M ionic strength $CaCl_2$ solutions, with swelling pressures below 20 kPa, possibly below the pressure sensor sensitivity with respect to friction forces).

Osmotic swelling is often considered as independent from exchanger population, which has not been shown theoretically or experimentally. The analysed data above indicate differences in various properties between Na and Ca forms also at low densities and high ionic strengths, where osmotic swelling is expected to govern swelling.

2.2. Coupling of exchanger population to swelling pressure and porosity at constant volume/dry density and ionic strength

Differences in swelling pressures between Na- and Ca-bentonites are well known and are attributed to different crystalline swelling, e.g. different hydration behaviour of the cations. Rapidly dissolving accessory minerals influence cation occupancy, and only data from purified bentonites or from montmorillonite should be compared at equal ionic strength. In most studies comparing swelling pressures or porosity distributions of Na- and Ca-montmorillonite, a homo-ionic treatment was done in suspension, where flocculation occurs in the Ca form only, and microstructural differences are to be still expected also in the compacted form produced from treated material. The cation exchange of a confined sample (by diffusion or by advection/diffusion) is time-consuming due to the comparably large CEC and small transport rates. The required long-term measurement of hydraulic conductivity and swelling pressure is therefore tedious and rather demanding. Short tests did likely not reach geochemical equilibrium and thus average a complex transient process.

Fig. 3 shows higher swelling pressures in Na-montmorillonite than in Ca-montmorillonite at densities below 800 kg/m^3 and below 3 M ionic strength. Pressures are higher in the Ca form at higher ionic strength. This trend continues with increasing densities, and at densities above 1600 kg/m^3, Ca-montmorillonite swelling pressures are higher at all ionic strengths considered.

A dual porosity concept implies that swelling pressure influences the porosity distribution. Kozaki et al. (2010) suggest equal interlayer spacings for Na- and Ca-montmorillonite at 1000 kg/m^3 dry density, as well as for mixed Na-Ca occupancies. In contrast, molecular dynamics studies indicate different d-spacings and swelling pressures for Na- and Ca-montmorillonite (Sun et al., 2015a, 2015b). Holmboe et al. (2012) found the same interlayer spacing (18.8 Å, three water layers) in both forms (700 kg/m^3), but could detect an additional low-angle reflection at 35–40 Å only in Na-montmorillonite (improved XRD set-up compared to Kozaki et al., 2010). This basal spacing is explained by osmotic swelling. The density at which the transition from crystalline to osmotic swelling occurs depends on the cation. If basal spacings of 40 Å are still considered as interlayer, Holmboe et al. (2012) suggest that the average interlayer distance of Na-montmorillonite is considerably higher than that of the Ca form (at 700 kg/m^3). Measurements on unconfined samples from the same authors also indicate larger basal spacings in Na-montmorillonite. This again agrees with lower hydraulic conductivities observed in Na-montmorillonite at this density (Fig. 3), caused by a lower advection-relevant free porosity fraction. The different behaviour of Na- and Ca-montmorillonite during purification and homo-ionic treatment questions the comparability of the two forms in a microstructural sense: the Ca form flocculates in dispersion, in contrast to the homogeneous dispersion of the Na form. This might lead to different grain or agglomerate sizes that persist and affect the microstructure after compaction. Differences in microstructure might lead to different hydraulic conductivities.

The experimental set-up of this study is chosen to measure swelling pressure and hydraulic conductivity at different cation occupancies and ionic strengths on the same confined bentonite core. A change of montmorillonite grain size or stacking number during Ca-Na exchange seems unlikely to occur in a highly compacted, confined sample. In this way we expect to achieve measurements that can be directly compared and any differences interpreted with more certainty.

3. Experimental method

Swelling pressure is commonly measured on compacted clay discs confined at constant volume (Karnland et al., 2003), with a prescribed dry density. Bottom and top of the bentonite disc are connected to an external reservoir through rigid flushed filters. The top filter transmits the force exerted by the swelling pressure to a force transducer. Each filter can be flushed with a peristaltic pump that circulates the external solution from one or two large reservoirs providing close to constant external pore water composition. This set-up is also used for diffusion experiments (Van Loon et al., 2007), but commonly without monitoring of swelling pressure. Advective flow may be driven by a hydraulic head gradient between the top and bottom filter and hydraulic conductivity

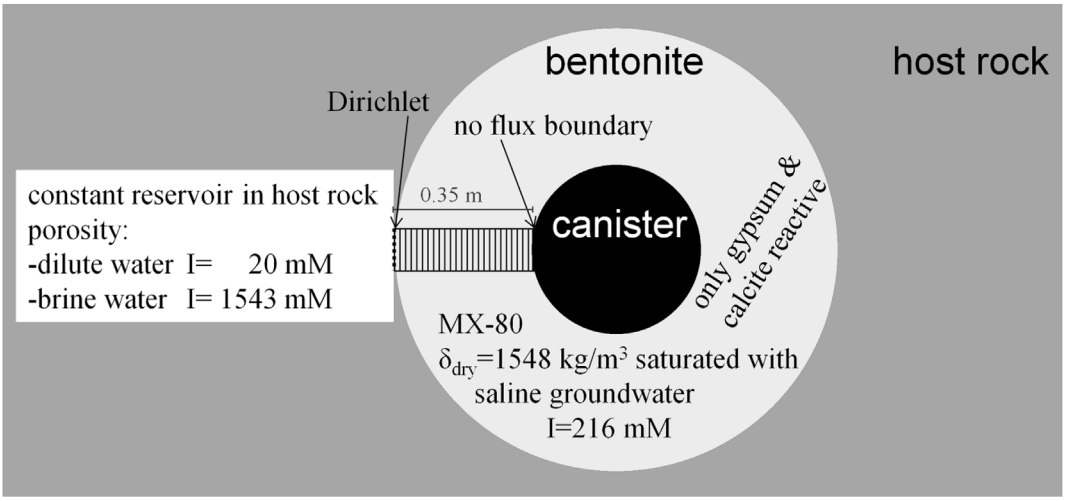

Fig. 4. Schematic of reactive transport model, key parameters and boundary conditions.

can be assessed according to Darcy's law (Karnland et al., 2006). The confining pressure measured by the force transducer can be considered to be equal to swelling pressure only at infiltration pressures far below the swelling pressure, and if friction forces can be neglected. The set-up including advection is complex in detail, because the hydraulic head gradient will lead to a gradient in pore pressure across the sample, and thus densities will redistribute accordingly, with higher porosity (lower density) at the inlet, and lower porosity (higher density) at the low-pressure side.

The advective set-up was used to measure hydraulic conductivity and swelling pressure in this study. MX-80 bentonite as received (12 wt. % water content relative to dry mass) was compacted to a dry density of 1470 kg/m^3, resulting in 43 vol% dry montmorillonite, 47 vol% porosity, 10 vol% accessory minerals, and an EMDD of 1335 kg/m^3 (calculated based on average phase densities). The corresponding disc has a diameter of 50 mm and a thickness of 12 mm. The external solution was infiltrated from the bottom with an infiltration pressure repeatedly set to 600 kPa and dropping to 200 kPa within 1–2 months. The exfiltrate at the top was captured repeatedly in syringes and sporadically analysed. Fluid volumes and the logged infiltration pressure were used to calculate the average hydraulic conductivity for a given time interval. After infiltration of approximately one pore volume, exfiltration of air at the top ceased, indicating full saturation. Subsequently, different electrolytes were infiltrated for a duration of 3.25 years.

4. Numerical model

Diffusive and advective multicomponent transport in Donnan and/or free porosity can be modelled with the finite difference code CrunchFlowMC based on the Nernst-Planck equation and Darcy's law (Steefel, 2009). Transport in the two porosity domains is combined with thermodynamic equilibrium speciation in the aqueous phase and kinetically controlled dissolution and precipitation of solids. The Donnan equilibrium defines the chemical composition of the Donnan porosity as a function of the free water composition, assuming equal activity coefficients in the two domains, but including the electrostatic correction in the Donnan domain based on the mean potential. The Donnan equilibrium replaces classical ion exchange models that are based on exchange capacity and distribution coefficients. All chemical equilibria and ion transport are solved simultaneously in one Jacobian matrix (global implicit approach). This dual porosity approach was benchmarked against other codes by Alt-Epping et al. (2014), who also provide more details.

Ionic strength in the free porosity defines the partitioning of total porosity into free porosity and Donnan porosity via the Debye length. The possible influence of the type of cation present in the Donnan porosity on the porosity distribution is not accounted for except for the ionic charge. Therefore, this approach cannot predict the outcome of the experiment in this study. Both, the interlayer distance and the thickness of the diffuse double layer are assumed to be equal and to depend linearly on the Debye length:

$$d = \lambda \frac{\beta}{\sqrt{I}} \tag{2}$$

with λ being the Debye length multiplier (< 1 in dense bentonites with overlapping Debye length in the interlayer), β a temperature-dependent physical constant, and I the ionic strength in the free pore water. λ is assumed to be constant at constant dry density and is derived from the montmorillonite basal spacing (and thus interlayer distance) measured by X-ray diffraction. Multiplying d with the total clay surface area (inner and outer) results in the *Donnan porosity*, and the *free porosity* is obtained by subtracting the Donnan porosity from the total porosity. This feature is currently implemented in a beta-version of CrunchFlowMC. Any porosity changes caused by this mechanism, but also by phase dissolution/precipitation, is intrinsically coupled to transport. Further details can be found in Yustres et al. (2017).

The modelling exercise presented here simplifies a chemically inert waste canister surrounded by a compacted MX-80 bentonite layer in contact with a porous host rock (Fig. 4). The host rock is an infinite reservoir represented by a Dirichlet boundary condition (fixed composition). A no-flux boundary represents the impermeable non-reactive canister surface on the other side of the bentonite, which is discretised in 1D into 25 cells. The bentonite is fully saturated with a saline groundwater (initial condition, 216 mM ionic strength, Yustres et al. (2017) contains complete chemistry). The model was independently calibrated with a Donnan porosity known from XRD measurements at equal dry density and at close to zero ionic strength (Holmboe et al., 2012). The derived multiplier λ was then kept constant and used to calculate the Donnan porosity at this saline groundwater ionic strength. The saturation at this elevated ionic strength leads to approximately 15 vol% Donnan and 30 vol% free porosity (eq. (2)). The response of the porosity to ionic strength might be overestimated, but data on interlayer thickness at such high ionic strengths are missing.

Two geological scenarios instantaneously convert the host rock's saline porewater into a brine (intrusion of a brine) or very dilute water (intrusion of glacial melt water). These two pore waters contact the bentonite at the host rock boundary and are modelled as two diffusion-only reactive transport simulations. Minor gypsum and calcite present in the bentonite are treated as kinetically reactive phases in the free porosity, all other minerals present are inert. A more detailed

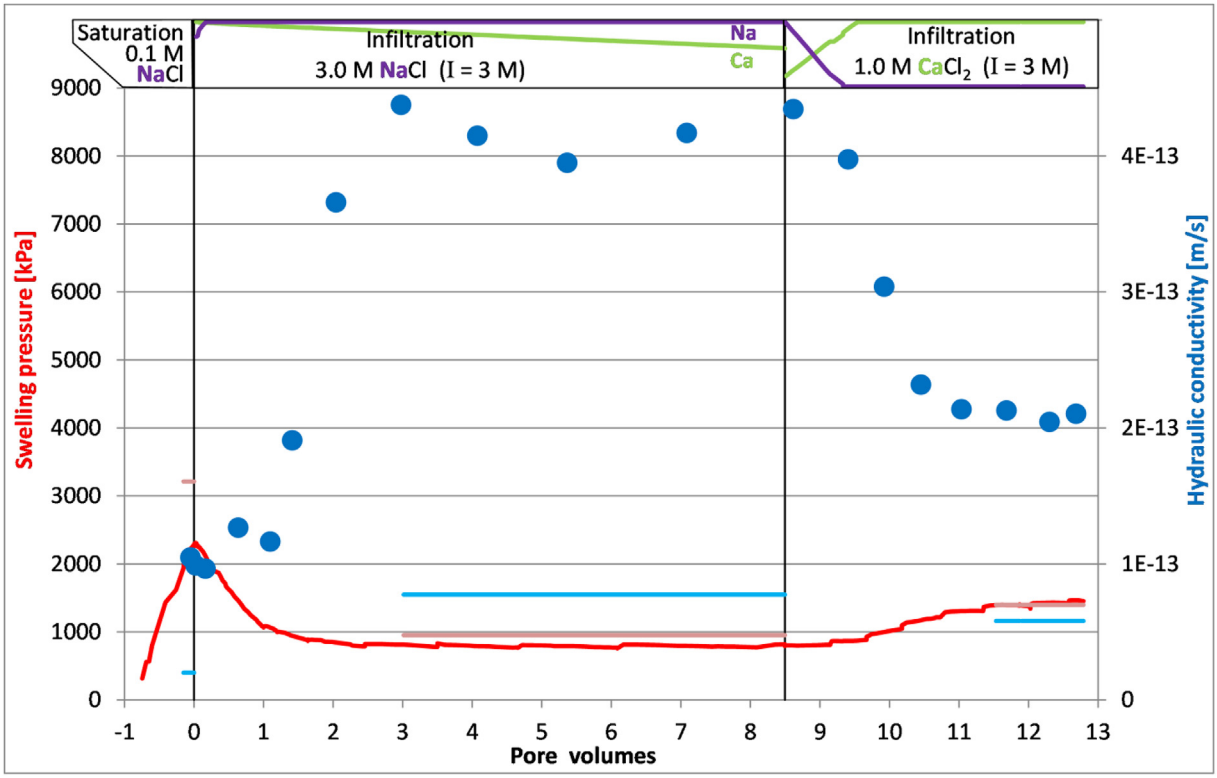

Fig. 5. Evolution of swelling pressure (red line) and hydraulic conductivity (blue circles) of a compacted MX-80 bentonite disc with infiltration of different electrolytes indicated at the top. The pale red and pale blue lines indicate values measured at equal EMDD by Karnland et al. (2006). The top graph indicates Na and Ca fractions of the total cation pool at equilibrium, estimated from simple mass balance considerations (see text for further explanation). One pore volume refers to the total water content in the bentonite disc, the 14 pore volumes required 3.25 years of infiltration at infiltration pressures in the range of 100–600 kPa. (For interpretation of the references to colour in this figure legend, the reader is referred to the Web version of this article.)

description of the water and solid compositions, transport parameters, and model parameters can be found in Yustres et al. (2017).

5. Experimental results

Hydraulic conductivity and swelling pressure measurements on a confined MX-80 bentonite disc compacted at 1470 kg/m^3 during and after exchange of its cation pool avoids the microstructural argument arising from sample treatment. Fig. 5 shows the initial saturation phase of the disc with 0.1 M NaCl (− 1 to 0 pore volumes of transport on the x-axis). Swelling pressure is lower and conductivity higher than measured by Karnland et al. (2006) on montmorillonite from MX-80 at equal EMDD. This may be explained with a still incomplete saturation at this early stage of the experiment and a free porewater ionic strength that is still higher than the infiltration solution: dissolution of accessory gypsum to equilibrium increases the ionic strength by 0.22 M. These processes may have led to a swelling pressure below the value obtained by Karnland.

After infiltrating 3 pore volumes of 3 M NaCl, swelling pressure and hydraulic conductivity are fairly constant. At 6 pore volumes, the outflow chemistry indicates complete gypsum removal and a Na-dominated exchanger occupancy. Swelling pressure is slightly below the value measured by Karnland et al. (2006), but hydraulic conductivity is about 5 times higher. This might be due to smaller samples (4.8 cm^3 vs. 23.6 cm^3), higher infiltration pressures (1000–2000 kPa vs. 400 kPa), and shorter measuring intervals (days vs. months) in the approach of Karnland et al. (2006). The measurements confirm the well-known HMC coupling of increasing ionic strength lowering swelling pressure and increasing conductivity. The top graph of Fig. 5 shows total cations in the disc (pore water and exchanger) as fraction of Ca present after saturation, and as fraction of complete Na occupancy (in equilibrium with 1 M NaCl). These values are estimated based on simple mass balance considerations (cation pool + infiltrating cations – exfiltrating cations). The graph shows that enough Na is supplied to reach fast equilibrium; in turn, the approx. 6 times smaller Ca pool is washed out much more slowly.

After infiltration of 1 M $CaCl_2$ (3 M ionic strength, equal to ionic strength of 3 M NaCl), the exchange of Na by Ca occurs comparably fast (based on the same mass balance estimation). In agreement, swelling pressure increases to a value matching measurements from Karnland et al. (2006). Hydraulic conductivity drops significantly, and stabilises at a value 3–4 times above that of Karnland et al. (2006).

6. Numerical modelling results

During 100 years of diffusive interaction of the bentonite with the dilute or brine water, porosity re-distribution proceeds differently. In case of the dilute groundwater (Fig. 6 left), the elevated ion content in the bentonite diffuses into the dilute host rock reservoir. This leads to a drop of ionic strength across the entire bentonite section, but more pronounced at the interface, where the Donnan porosity expands drastically at the expense of free porosity. Due to slower diffusion in this expanded Donnan porosity and partial anion exclusion, the overall equilibration process slows down considerably. The core is still far from equilibrium after 100 years of contact with the dilute reservoir. In contrast, the high ionic strength brine diffuses into the free porosity of the bentonite section, which leads to a decrease of the Donnan porosity (Fig. 6 left). This enlarges the free porosity and provides a faster pathway for both anions and cations. Therefore, this bentonite has reached equilibrium within 100 years of interaction with the brine reservoir, neglecting the comparatively small influence of reactive accessory minerals on the pore water composition.

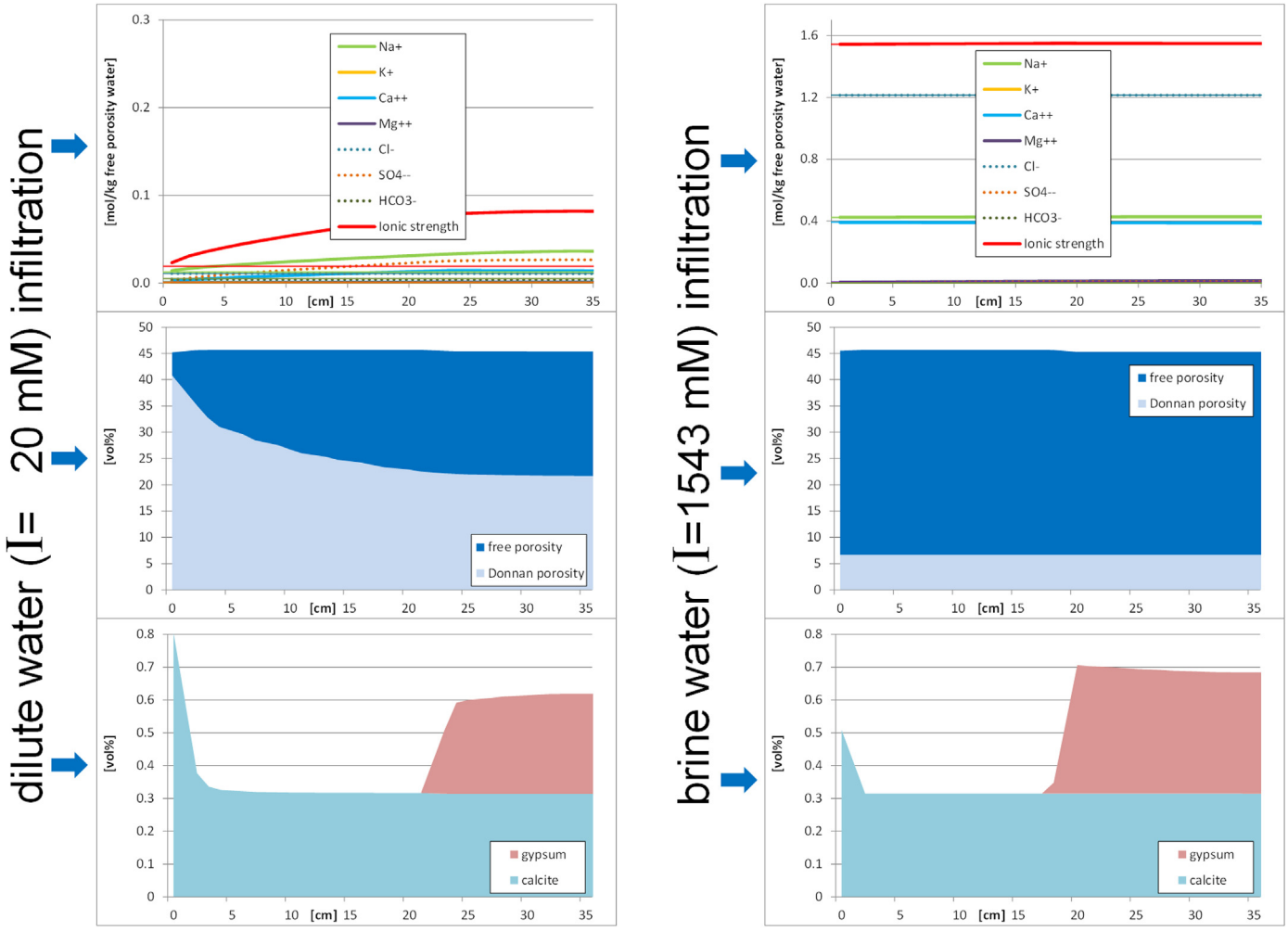

Fig. 6. Profiles across a bentonite layer in contact with dilute water (left) and brine water (right) after 100 years of interaction. Concentrations in free pore water (top), porosity fractions (middle), and reactive mineral volume fractions (bottom).

The presence of gypsum and calcite, the only solids considered as reactive in this approach, adds some complexity to the system: the small amount of gypsum present initially (0.4 vol%) dissolves, and sulphate and Ca leave the bentonite. No drastic difference between the two scenarios is predicted: although transport out of the bentonite is faster in case of the brine water, slightly more gypsum is still present after 100 years. The dilute water is slightly more saturated with respect to gypsum than the brine water, but both waters are undersaturated. Therefore, differences in gypsum leaching arise not only from the dissimilar transport in the two cases, but also from different dissolution rates (fastest at far-from-equilibrium conditions). In contrast, calcite precipitates at the reservoir-bentonite interface: both, dilute and brine water are slightly oversaturated with respect to calcite, which leads to this slow calcite precipitation in the bentonite next to the interface. Calcite precipitation in the host rock, represented by a constant-concentration boundary, is not considered in this approach.

7. Discussion

The swelling pressures at different ionic strengths and cation occupancy measured in this study agree well with literature data. Hydraulic conductivity clearly responds to changes in ionic strength, and to exchange of Na with Ca at equal ionic strength. A drastic change of the microstructure, like agglomeration or changes in smectite grain size or stacking number, seems unlikely in this compacted and confined state. An increase in interlayer distance (and therefore Donnan porosity) at the expense of free porosity providing the main flow-active domain, seems a more plausible cause for the decreasing conductivity.

Further experimental data from literature support this explanation via pore size redistribution for changes in solute transport. Choi and Oscarson (1996) consistently measured higher HTO, I^-, and Sr^{2+} diffusive fluxes across purified Ca-exchanged Avonlea bentonite than across the Na form (both at 1300 kg/m^3 dry density). They attribute these differences to the larger particle size and therefore greater portion of larger pores in Ca-bentonite. This interpretation is supported by mercury intrusion porosimetry, which shows a distinct fraction of 1 μm pores in Ca-bentonite that is missing in the Na-form. Kozaki et al. (2010) derived apparent diffusion coefficients for HTO and $^{45}Ca^{2+}$ across Na- and Ca-montmorillonite mixtures with different ionic equivalent fractions of Ca^{2+} ions at a dry density of 1000 kg/m^3. The apparent diffusion coefficient of HTO increased slightly with an increase in the ionic equivalent fraction of Ca^{2+}, but the coefficients for $^{45}Ca^{2+}$ remained in the same range. An increase in the proportion of the faster free porosity pathway with higher ionic strength can explain the HTO behaviour, whereas additional processes like Ca^{2+}/Na^+ redistribution between Donnan and free porosity or in the Stern layer complicate the interpretation in case of cations like $^{45}Ca^{2+}$.

No direct measurements of Na-/Ca-montmorillonite (or other mixed cations) basal spacings at higher densities (crystalline swelling region) could be found. But differences in hydraulic conductivity and swelling pressure at high densities frequently reported in literature suggest also an effect of the cation population on pore geometry.

Li^+ occupancy can lead to a substantial decrease in swelling pressure, especially at elevated temperatures. This phenomenon is not caused by the presence of Li^+ in the interlayer, but attributed to the incorporation of Li^+ into octahedral vacancies in the smectite TOT layer, which then decreases layer charge, CEC, and therefore swelling pressure. This mechanism can be used to determine the smectite content (Greene-Kelly, 1953, 1955). It is still controversial if Cu^+, or Cu^{2+}, can also enter the vacancies at repository temperatures due to the small ion radii similar to Li^+. Copper is a proposed canister (massive or thick coating) material in several concepts, and its corrosion releases copper cations, and may thus alter smectite very near to the canister. The effect of these cations on swelling pressure may be of different nature than the effect of Ca-Na exchange.

The modelling exercise does not aim for the prediction of the experimental data measured in this study. In its current state, the model cannot capture the effect of Na-Ca exchange on transport in bentonite. The experimental data rather support the effect of chemistry on the pore size distribution, which in turn affects solute transport. This is the underlying coupling implemented in the code so far for ionic strength effects. Implementation of the cation occupancy effect is delayed by the scarce amount of consistent data available, but is a subject of ongoing research.

What is also lacking in this model is a mechanical coupling between changes in porosity distribution (and thus swelling pressure) and mass re-distribution that will over time even out differences in local swelling pressures. Including such a coupling would tend to soften the gradients presented in our simplified model to some extent. An example of such a fully coupled HMC model is discussed in Yustres et al. (2017).

The outcome of the model including two extreme cases of changes in external chemical composition demonstrates that the ionic strength of a groundwater in contact with the saturated bentonite buffer significantly influences solute transport in the buffer. Equilibration time of the buffer with the external solution is significantly prolonged in case of a low salinity groundwater contacting the buffer. The low ionic strength leads to a drastic increase of the Donnan porosity at the expense of the free porosity. Because the latter provides the faster pathway for diffusive solute transport, the faction of free porosity directly controls the fluxes of all species. As soon as ionic strength drops in the buffer close to the interface, free porosity fraction also drops, which leads to a bottleneck for the remaining solutes in the buffer. In contrast, Donnan porosity (and swelling pressure) collapse in contact with the high ionic strength brine, free porosity expands and provides a fast pathway for in-diffusion of the high salinity.

8. Conclusions

Although the influence of the chemical environment on the bentonite's swelling pressure and hydraulic conductivity is recognised in literature, the resultant HMC coupling is largely neglected in geomechanical or geochemical modelling. Only one consistent data set exists (Karnland et al., 2006) that describes the relationship between swelling pressure, hydraulic conductivity, cation occupancy, and external solution composition (equilibrated with the bentonite) at specified EMDD (effective montmorillonite dry density). This dataset implies swelling pressures decreasing by up to a factor of three with increasing ionic strength (0.1 M-3 M), or with exchange of Ca for Na. Simultaneously, hydraulic conductivities increase by up to a factor of four. A detailed quantitative understanding of this coupling is presently lacking. Inconsistencies in hydraulic conductivity exist among different data sets and hint at inherent experimental challenges but are presently not resolved.

Information gained on pore distribution as a function of the chemical environment at constant-volume and in a confined state (swelling pressure) would be most valuable for further progress on quantifying HMC coupling. This may be achieved via measurements of interlayer spacing under such controlled conditions. A commonly employed method for measuring porosity distribution used in soil science is mercury injection porosimetry. It has to be performed on dried samples, and dried samples have lost most water from smectite interlayers and therefore most of the pore space has re-arranged and does not reflect the saturated state.

Only one study documents a dependency of interlayer distance on ionic strength (Kozaki et al., 2008). An effect of cation occupancy on interlayer distance has not been directly observed so far. However, porosity redistribution can qualitatively explain the response of transport properties and also of anion exclusion to the chemical environment.

The implementation of porosity redistribution into reactive transport codes is a first step towards a quantification of HMC coupling. A first approach based on Debye length predicts a significantly slower equilibration with a low ionic strength solution than with a high salinity solution. This approach very likely overestimates the response of porosity redistribution to ionic strength. The rigorous application of eq. (2) at very low ionic strength leads to a Donnan porosity which exceeds the total porosity and is therefore too simple a relationship. The influence of dissolution/precipitation of accessory minerals (e.g., gypsum, calcite) is comparatively small and insignificant for the evolution of the transport properties.

More well constrained and complete experimental data are needed for a better understanding of HMC coupling in bentonite. Fitting of such data will result in empirical relationships for a specific bentonite material. These parameterisations can be implemented into HMC coupled reactive transport models. Such tools would be helpful to explore the overall effects and significance of these coupling terms for some relevant scenarios.

Acknowledgements

Partial funding by Nagra and Posiva is kindly acknowledged. The implementation of HMC coupling into CrunchFlowMC was done by Carl Steefel.

References

Alt-Epping, P., Tournassat, C., Rasouli, P., Steefel, C.I., Mayer, K.U., Jenni, A., Mäder, U., Sengor, S.S., Fernández, R., 2014. Benchmark reactive transport simulations of a column experiment in compacted bentonite with multispecies diffusion and explicit treatment of electrostatic effects. Comput. Geosci. 1–16.

Birgersson, M., Karnland, O., 2009. Ion equilibrium between montmorillonite interlayer space and an external solution-Consequences for diffusional transport. Geochem. Cosmochim. Acta 73, 1908–1923.

Chen, Y.-G., Zhu, C.-M., Ye, W.-M., Cui, Y.-J., Wang, Q., 2015. Swelling pressure and hydraulic conductivity of compacted GMZ01 bentonite under salinization–desalinization cycle conditions. Appl. Clay Sci. 114, 454–460.

Choi, J.W., Oscarson, D.W., 1996. Diffusive transport through compacted Na- and Ca-bentonite. J. Contam. Hydrol. 22, 189–202.

Christidis, G.E., Blum, A.E., Eberl, D.D., 2006. Influence of layer charge and charge distribution of smectites on the flow behaviour and swelling of bentonites. Appl. Clay Sci. 34, 125–138.

Dixon, D.A., Chandler, N.A., Baumgartner, P., 2002. The influence of groundwater salinity and interfaces on the performance of potential backfilling materials, 6th International Workshop on Design and Construction of Final Repositories. ONDRAF/NIRAS, Brussels, Belgium.

Glaus, M.A., Frick, S., Rosse, R., Van Loon, L.R., 2010. Comparative study of tracer diffusion of HTO, Na-22(+) and Cl-36(-) in compacted kaolinite, illite and montmorillonite. Geochem. Cosmochim. Acta 74, 1999–2010.

Greene-Kelly, R., 1953. Irreversible dehydration in montmorillonite. Part II. Clay Miner. Bull. 58, 52–65.

Greene-Kelly, R., 1955. Dehydration of montmorillonite minerals. Mineral. Mag. 30, 604–615.

Güven, N., 1988. Smectites. Rev. Mineral. 19, 497–559.

Holmboe, M., Wold, S., Jonsson, M., 2012. Porosity investigation of compacted bentonite using XRD profile modeling. J. Contam. Hydrol. 128, 19–32.

Jenni, A., Gimmi, T., Alt-Epping, P., Mäder, U., Cloet, V., 2017. Interaction of ordinary Portland cement and Opalinus Clay: dual porosity modelling compared to experimental data. Phys. Chem. Earth, Parts A/B/C 99, 22–37.

Jenni, A., Mäder, U., Fernández, R., 2014. Multi-component Advective-diffusive Transport Experiment in MX-80 Compacted Bentonite: method and Results of 2nd Phase of Experiment and Post Mortem Analysis. Arbeitsbericht NAB 14-22. Nagra, Wettingen, Switzerland.

Karnland, O., 2010. Chemical and Mineralogical Characterization of the Bentonite Buffer for the Acceptance Control Procedure in a KBS-3 Repository. Technical Report TR-10-60. SKB, Stockholm, Sweden. www.skb.se.
Karnland, O., Muurinen, A., Karlsson, F., 2003. Bentonite swelling pressure in NaCl solutions – experimentally determined data and model calculations. In: Alonso, E.E., Ledesma, A. (Eds.), International Symposium on Large Scale Field Tests in Granite. Taylor & Francis Group, Barcelona.
Karnland, O., Olsson, S., Nielsson, U., 2006. Mineralogy and Sealing Properties of Various Bentonites and Smectite-rich Clay Materials. Technical Report TR-06-30. SKB Stockholm, Sweden. www.skb.se.
Kaufhold, S., Baille, W., Schanz, T., Dohrmann, R., 2015. About differences of swelling pressure - dry density relations of compacted bentonites. Appl. Clay Sci. 107, 52–61.
Kozaki, T., Liu, J., Sato, S., 2008. Diffusion mechanism of sodium ions in compacted montmorillonite under different NaCl concentration. Phys. Chem. Earth 33, 957–961.
Kozaki, T., Sawaguchi, T., Fujishima, A., Sato, S., 2010. Effect of exchangeable cations on apparent diffusion of Ca(2+) ions in Na- and Ca-montmorillonite mixtures. Phys. Chem. Earth 35, 254–258.
Kumpulainen, S., Kiviranta, L., 2011. Mineralogical, chemical and physical study of potential buffer and backfill materials from ABM test package 1. In: Posiva (Ed.), Working Report. B+Tech Oy, Eurajoki. Finland.
Meunier, A., 2005. Clays. Springer, Berlin.
Seiphoori, A., Ferrari, A., Laloui, L., 2014. Water retention behaviour and microstructural evolution of MX-80 bentonite during wetting and drying cycles. Geotechnique 64, 721–734.
Steefel, C.I., 2009. Crunch Flow: software for Modeling Multicomponent Reactive Flow and Transport. Berkley, USA. http://www.csteefel.com.
Sun, L.L., Hirvi, J.T., Schatz, T., Kasa, S., Pakkanen, T.A., 2015a. Estimation of montmorillonite swelling pressure: a molecular dynamics approach. J. Phys. Chem. C 119, 19863–19868.
Sun, L.L., Tanskanen, J.T., Hirvi, J.T., Kasa, S., Schatz, T., Pakkanen, T.A., 2015b. Molecular dynamics study of montmorillonite crystalline swelling: roles of interlayer cation species and water content. Chem. Phys. 455, 23–31.
Van Loon, L.R., Glaus, M.A., Müller, W., 2007. Anion exclusion effects in compacted bentonites: towards a better understanding of anion diffusion. Appl. Geochem. 22, 2536–2552.
Yustres, A., Jenni, A., Asensio, L., Pintado, X., Koskinen, K., Navarro, V., Wersin, P., 2017. Comparison of the hydrogeochemical and mechanical behaviours of compacted bentonite using different conceptual approaches. Appl. Clay Sci. 141, 280–291.
Zhu, C.-M., Ye, W.-M., Chen, Y.-G., Chen, B., Cui, Y.-J., 2013. Influence of salt solutions on the swelling pressure and hydraulic conductivity of compacted GMZ01 bentonite. Eng. Geol. 166, 74–80.